Stability of ZnMgO oxide in a weak alkaline solution

E. Diler[1,2], S. Rioual[1], B. Lescop[1], D. Thierry[2], and B. Rouvellou[1]

[1] Laboratoire de Magnétisme de Bretagne, EA 4522, CNRS, Université de Brest, UBO, 6 av. Le Gorgeu, 29285 Brest Cedex, France

[2]Institut de la Corrosion, 220 rue Pierre Rivoalon, 29200 Brest, France

Abstract

Zinc oxide (ZnO) is a chemical compound of great interest used, for example, as photocatalyst in the purification of wastewater or polluted air. However, neither dissolution, nor photo-dissolution of ZnO is negligible: indeed, both processes reduce significantly the efficiency of photocatalysis and then lead to a secondary pollution by free Zn^{2+}. In the present study, the stability of ZnMgO thin films in weak alkaline solution is investigated. We demonstrates that the replacement of Zn^{2+} ion with Mg^{2+} ion results in the production of a $Zn_{0.84}Mg_{0.16}O$ solid solution, whose stability is higher than that of the ZnO sample. This alloy, thus, constitutes an alternative to the use of ZnO in photocatalysis applications. To gain more insights into the higher resistance of such alloys to the dissolution process, X-Ray photoelectron spectroscopy measurements were performed. They highlighted the role of OH group adsorption in the experimentally observed enhancement of ZnMgO stability.

Keywords: Zinc oxide; ZnMgO Solid solution; Dissolution; Photo-dissolution

Corresponding author : Dr. S. Rioual
Email address: rioual@univ-brest.fr
Fax number: + 33 (0)2 98 01 64 39

1. Introduction

Zinc oxide (ZnO) is an n-type wide-band gap semiconductor with a high exciton binding energy. Because of its interesting multi-functionality, over the last few years it was the subject of extensive studies for applications in gas sensors, solar cells, photodetectors, light emitting diodes, magnetic storage and photocatalysis. In some cases, ZnO has displayed a greater efficiency in photocalysis than TiO_2, which is generally considered as the most suitable photocatalyst [1]. With respect to the other photocatalytic materials, the emitting properties of ZnO are unique and enable one to create catalytic systems to simultaneously detect and destroy environmental organic contaminants [2]. However, its use in photocatalysis is limited by two parameters: Firtsly, as it is activated under UV irradiation because of its large band gap of 3.3 eV ($\lambda \approx 380$ nm), only about 5% of the photons received by natural light illumination can be used in the photocatalytic reactions. The second drawback is its instability in aqueous media due to photocorrosion by UV irradiation. Investigations by Spathis and Poulios have dealt with the corrosion of Zn and ZnO [3]: in particular, these authors observed a quicker formation of corrosion products under illumination. This behaviour was explained by the formation of an electron-hole pair produced by photoexcitation and responsible for an enhancement of dissolution. Recently, a more extensive study about ZnO stability [4] demonstrated that the greater stability displayed by ZnO near pH=9.9 was explained by the formation of $Zn(OH)_2$ hydroxide, which limits Zn dissolution. At such a pH level, the low solubility of $Zn(OH)_2$ protects ZnO from further reaction with OH^- and dissolution.

Different methods were, recently, initiated to suppress the photodissolution process. They include organic coating [5] and surface hybridisation with carbon [6]. Instead of protecting only the surface that can be oxidised and thus damaged, a solution would be to elaborate compounds with higher photocatalytic properties and better photocorrosion

resistance. Recently, doping of ZnO with Mg^{2+} proved to lead to an enhancement of photocatalytic efficiency [7]. Many methods have been developed so far in order to produce ZnMgO thin films, e.g. pulsed laser deposition [8], RF and DC sputtering [9,10] and spray pyrolysis [11-13]. In the present work, we use the spray pyrolysis method, a versatile low cost technique which enables deposition onto large areas. However, in contrast to ZnO, no investigation about the stability of this oxide is available in the literature. Here, focus is on the stability of $Zn_{(1-x)}Mg_{(x)}O$ oxides in a weak alkaline solution, where ZnO displays a relatively low dissolution rate, and may, thus, be used as a photocatalyst. After a physico-chemical characterisation of the samples under study, we will show in the present work that ZnMgO is more stable than ZnO, and then discuss the origin of this behaviour.

2. Experimental details

2.1. Preparation

To produce $Zn_{(1-x)}Mg_{(x)}O$, Zinc acetate dihydrate ($Zn(CH_3COO)_2.2H_2O$, Alpha Aesar) and Magnesium acetate tetrahydrate ($Mg(CH_3COO)_2.4H_2O$, Alpha Aesar) were dissolved in demineralised water with magnesium at different concentrations varying from 0% to 16%. For the enhancement of the film growth and to avoid zinc hydroxide precipitation in solution, the pH was adjusted to pH= 4.5 by addition of a small quantity of acetic acid [14]. The final solution was pulverised using compressed air at a distance of 50 cm on the 500°C-heated substrate (conductive tin-doped indium oxide or glass). The flow rate was 3.3 ml/min.

2.2. Characterisation

The sample film thickness was determined by: i) weighing the samples before and after deposition and ii) inductively-coupled plasma atomic emission (ICP). The glass substrates were weighed 5 times before and after deposition with a precision weighing balance, Genius series from Sartorius. The thickness of the thin film was estimated from the

density of the zinc oxide (d = 5.606 g/cm^3). For ICP measurements, ZnO films were let to dissolve for 30 min in a saturated solution of glycine placed in an ultrasonic bath, and then analysed.

The crystalline structure of the different films was analysed in (θ-2θ) configuration by X-ray diffraction (XRD) with a Brucker apparatus using the CuKα radiation. The compositions of the different films were determined by depth-profile X-Ray photoelectron spectroscopy (XPS) according to the procedure described elsewhere [15]. XPS apparatus was also used to measure the secondary electron energy spectra by polarising the sample by 10 V with respect to the analyser. The surface topography was studied by Atomic Force Microscopy (AFM) (Veeco, NanoScope V) in tapping mode using commercial P doped Si tip (Veeco, RTESP). The optical properties in the 200–1100 nm wavelength range were analyzed using UV–visible spectrometry with a Jasco apparatus. The resistivity was measured by the four-point probe technique in the air and in a vacuum chamber at about 10^{-1} Pa.

The stability of the thin films was investigated in a solution of borax at pH 8.4 to keep the pH at a fixed value, between 7 and 10, where dissolution is expected to be rather low. After immersion of the thin film in this solution, the open circuit potential (OCP) was measured with a leak-free saturated Ag/AgCl electrode as reference and a multi channel data logger (EPC8 from NKE). These measurements were made over several days under the direct illumination of the sun.

3. Results and discussion

3.1. Characterisation of the $Zn_{1-x}Mg_xO$ alloys

Characterisation of the $Zn_{1-x}Mg_xO$ films for magnesium concentration, *x*, in the range 0 to 16% led to thickness of 200 ± 10 nm. Figure 1 displays the transmittance measurements. For the direct band gap materials, the relationship between the absorption coefficient, α, and

the photon energy, hν, can be expressed as follows [16]: $\alpha h\nu = A(h\nu - E_g)^{1/2}$, where E_g is the band gap. The determination of the band gap of the $Zn_{1-x}Mg_xO$ oxide films showed a linear variation from 3.22 to 3.42 eV with x. This relatively weak increase with Mg concentration should not lead to a deterioration of the photocatalytic efficiency of ZnMgO with respect of ZnO.

The XRD patterns of the films displayed an intense (002) peak at about 34.5° with additional small (100) and (101) features located at 31.8° and 36.3° respectively. These lines (not shown here) are indicative of the polycrystalline würtzite structure of the films. This crystallographic structure was still observed even at the 16% Mg concentration with no MgO-associated pattern. This is in agreement with other studies that have shown the presence of würtzite structure up to 40% Mg concentration [17]. The higher (002) peak displayed on Fig. 2 indicates that the preferential orientation for the film is along the c-axis. One should also note the Mg-doping-induced shift of this peak towards high angles: it corresponds to a lattice compression caused by the replacement of Zn^{2+} by Mg^{2+} with its associated decrease in the ion radius from 0.60 to 0.57 Å. This behaviour consistent with band gap results is characteristic of a solid solution and has been previously reported on ZnMgO thin films produced by either spray pyrolysis [12,13] or pulse laser deposition (PLD) [18]. It is worth noting that this shift was neither visible on XRD patterns from powders [19] nor predicted by recent electronic structure calculations [20]. This disagreement is likely explained by the number of defects within the samples and, thus, by the method in use for their preparation.

The composition of $Zn_{1-x}Mg_xO$ for x = 0 and 0.16 was determined by XPS on using an AlKα source. Zn(2p), Mg(1s) and O(1s) spectra were measured and fitted by CasaXPS software to calculate their integral. By correcting these values by the Scofield factors and the inelastic mean free paths of the detected photoelectrons, the stoechiometry of the compounds was determined. The dopant concentrations in the solution and within the film were found to

be in good agreement. Figure 3 displays the O(1s) spectrum of ZnO and $Zn_{0.84}Mg_{0.16}O$. For ZnO, the two components contributing to the spectrum at 529.9 and 531.8 eV correspond to ZnO and OH groups at the surface, respectively. The latter feature was previously observed on PLD-produced ZnO and explained by the dissociation of adsorbed water at the surface [18]. Thorough investigations by Almeida *et al.* [21] showed that this process is governed by the number of defects, e.g. oxygen vacancies, within the oxide under study.

The electrical resistivity was measured by the following equation:

$$\rho = R_s t \frac{\pi}{\ln 2} \quad (1)$$

Where ρ is the resistivity, R_S is the sheet resistance and t the sample thickness. The resistivity values of undoped ZnO measured in the air and at 10^{-1} Pa were 820 and 4 Ωcm, respectively. Such a vacuum dependence of the resistivity can be explained by the capture of the electrical charges at the surface by hydroxyl groups as explained in Ref. [22]. It, thus, confirms the importance of water adsorption in this study. The comparison of the resistivity values of ZnO and of $Zn_{0.84}Mg_{0.16}O$ samples measured in air showed an increase from 820 to 9.10^5 Ωcm. For intermediate Mg doping ratios (x=0, 0.02, 0.04, 0.08, 0.16), one observes a continuous increase of the resistivity with the x doping. This increase is in agreement with Yoshino *et al.* [12] and is consistent with the stronger contribution of the OH peak observed in our XPS measurements for $Zn_{0.84}Mg_{0.16}O$ with respect to ZnO. One should note that, in Ref. [18], the significant contribution of the OH peak in XPS spectrum was explained by the porous character of the PLD-produced ZnO. In the present study, as shown in figure 4 by AFM measurements, the strong water adsorption can be explained by the microstructure of the surface composed of numerous grains of about 60 nm: OH adsorption is, thus, promoted by the large surface/bulk ratio. Both surfaces display similar roughness and microstructure

leading to the hypothesis that the chemical nature of the thin films plays also an important role in the OH adsorption.

3.2. Stability of the Mg-based solid solution

The recent use of open-circuit potential (OCP) measurement as an indicator of the damage of photoactive materials in aqueous solutions [23] drove us to make such measurements of ZnO and $Zn_{0.84}Mg_{0.16}O$ in a borax solution at pH = 8.4 and under natural night/day cycles. The results presented in Fig. 5(a) are about samples exposed to cyclic illuminations, and those in Fig. 5(b) deal with samples placed under dark conditions for 5 days and then exposed to natural night/day cycles. For short exposure times, both figures show equilibrium between the Fermi level and the redox couple of the electrolyte at about 35 mV vs Ag/AgCl. Light exposure causes a shift of OCP by about 330 mV towards negative values. This can be explained by the light-induced creation of the electron-hole pairs and the subsequent creation of an additional photovoltage. The latter is due to the separation of both charges and to the low recombination rate within the material. In the dark, the OCP comes back immediately to its initial magnitude (35 mV vs Ag/AgCl). After few days in the borax solution, Figure 5(a) clearly shows a reduction of ZnO-OCP amplitude with respect to that of ZnMgO. Figure 5(b) presents the same behaviour, but with a delay of about 5 days since the samples was exposed later to the light, showing that the integrated time of illumination is the key parameter of the ZnO degradation. These results give thus evidence of both: i) the relevance of ZnO films degradation by light irradiation and ii) the greater stability of ZnMgO with respect to ZnO.

To investigate the modification of the thin films after borax immersion, XPS measurements were carried out. An argon ion sputtering at 1.5 keV with a sputtering rate of about 0.5 nm/minute was used to investigate the chemical environment of thin film elements

throughout its thickness. Figure 6(a) illustrates the O(1s) spectra obtained for different sputtering times. The difference observed in the shape of the outer surface layer O(1s) spectrum measured at t=0 min with respect to the other ones is explained by strong carbon contamination of the surface. In the inner part of the film, two components at about 530.2 and 532.4 eV contribute to the O(1s) spectrum. As discussed above, they are explained by Zn-O-Zn bonds and OH species, respectively. A comparison of figures 6(a) and 3 shows that, after a stay in borax, the contribution of OH species is: i) definitely stronger than previously and ii) not limited to the surface region.

For both films, the OH peak presents a decreasing amplitude from the surface to the inner part of the film where the ZnO and ZnMgO oxides are localised. As shown in figure 6(b), this decrease of the OH contribution is confirmed by an increase of the Zn and Mg contents in the inner part of the film with respect to the surface. The measurements of the secondary electrons spectra of ZnO presented in figure 6(c) show an increase of the work function of the surface with respect to the inner part of the film; this is indicative of the changes in the composition of the film observed in figure 6(a) and 6(b). The observed high value of the work function induced by the hydroxide formation in the first nanometer range reduces the charge transfer rate at the liquid/solid interface and then prevents the dissolution of the underlying substrate. Furthermore, in figure 6(a), as found already before immersion of the samples in borax, the inclusion of Mg in ZnO leads to an enhancement of hydroxide concentration. This observation could be correlated to the slight increase of the work function of ZnMgO with respect to ZnO as displayed in figure 6(c).

Immersion of a sample in borax for a certain time permits the development of several reactions at its surface. Among them, the creation of $Zn(OH)_2$ film on ZnO is suspected to represent the predominant reaction in the dark [4]. This is explained by the low solubility of $Zn(OH)_2$ in a weak alkaline solution. This scenario is confirmed by our XPS results. The

results presented above deal with the relative stability of ZnMgO with respect to ZnO. OCP measurements (Fig. 5) showed indeed that ZnMgO thin films were definitely more stable than ZnO in a weak alkaline solution. However, the exact role of Mg in the protection of ZnMgO against corrosion is a rather complex phenomenon and needs further clarification. The higher band gap of Mg-doped ZnO compared to ZnO (Fig. 1) suggests the implication of a lower number of photons in the creation of electron/hole pair with its consecutive reduction of photocorrosion in the doped Mg alloy. However, the amplitude of OCP being almost alike for the two kinds of materials, the numbers of holes created by irradiation are rather similar. It is likely that this parameter is not the main factor at the origin of the greater stability of the Mg-doped ZnO. The second difference observed in figure 3 and 6(a) between both materials concerns the OH enrichment of the ZnMgO surface with respect to ZnO after immersion in the borax solution. To further discuss this point, we present in Table 1 the OH/O ratio measured from the decomposition of the O(1s) spectra for both ZnO and ZnMgO samples; and finally the increase of the OH content in the last column. As shown in this table, this increase is definitely higher than the increase of 16% due to magnesium doping. This is explained by the complex nature of the hydroxide layer which is not a simple mixture of $Zn(OH)_2$ and $Mg(OH)_2$ but which should contains hydroxides such as $Zn_{1-x}Mg_x(OH)_2$. The different nature of these hydroxides combined with their higher content are thus at the origin of the observed better stability of ZnMgO. The strong OH adsorption may result from the stabilization of the ZnMgO surface. A theoretical investigation of the chemistry of ZnMgO oxide surface with respect to ZnO would certainly give further information on this point. Finally, one should note that the observed enhancement of OH amount and the resulting greater stability of ZnMgO, are both in agreement with studies made on the corrosion resistance of ZnMg metallic alloys, where their greater resistance to corrosion compared to Zn was explained by the formation of hydroxide [24,25].

4. Conclusion

Solid solutions of $Zn_{1-x}Mg_xO$ with x lying within 0 and 16% were produced by spray pyrolysis. Increase of Mg content led to both the keeping of the würtzite structure for ZnO and the decrease of the lattice parameter. OCP measurements allowed us to investigate the stability of the samples in borax at pH = 8.4, and ZnMgO proved to be more stable than ZnO. This behaviour is attributable to the important contributions of OH species in the very first nanometers just below the surface and proves that ZnMgO is a better candidate for catalytic applications than ZnO.

Acknowledgment

The authors acknowledge C. Calvarin for his contribution in the design of the spray pyrolysis device and P. Elies for AFM measurements.

References

[1] K. Gouvea, F. Wypych, S.G. Moraes, N. Durian, N. Nagata, P. Peralta-Zamora, Semiconductor-assisted photocatalytic degradation of reactive dyes in aqueous solution , Chemosphere 40 (2000) 433-440.

[2] P.V. Kamat, R. Huehn, R. Nicolaescu, A Sense and Shoot Approach for Photocatalytic Degradation of Organic Contaminants in Water, J. Phys. Chem. B 106 (2002) 788-794.

[3] P. Spathis, I. Poulios, The corrosion and photocorrosion of zinc and zinc oxide coatings, Corr. Sci. 37 (1995) 673-680.

[4] J. Han, W. Qiu, W. Gao, Potential dissolution and photo-dissolution of ZnO thin films, J. Hazard. Mat. 178 (2010) 115-122.

[5] R. Comparelli, E. E. Fanizza, M.L. Curri, P.D. Cozzoli, G. Mascolo, A. Agostiano, UV-induced photocatalytic degradation of azo dyes by organic-capped ZnO nanocrystals immobilized onto substrates, Appl. Catal. B: Env. 60 (2005) 1-11.

[6] Y. Li, X. Zhou, X. Hu, X. Zhao, P. Fang, Formation of Surface Complex Leading to Efficient Visible Photocatalytic Activity and Improvement of Photostabilty of ZnO, J. Phys. Chem. C 113 (2009) 16188-16192.

[7] X. Qiu, L. Li, J. Zheng, J. Liu, X. Sun, G. Li, Origin of the Enhanced Photocatalytic Activities of Semiconductors: A Case Study of ZnO Doped with Mg2+, J. Phys. Chem. C 112 (2008) 12242-12248.

[8] W. Yang, R.D. Vispute, S. Choopun, R.P. Sharma, T. Venkatesan, and H. Shen, Ultraviolet photoconductive detector based on epitaxial Mg0. 34Zn0. 66O thin_films. Appl. Phys. Lett., 78 (2001) 2787-2789.

[9] H. Li, Y. Zhang, X. Pan, T. Wang, and E. Xie. The effects of thermal annealing on properties of MgxZn1-xO films by sputtering. J. of All. and Comp., 472 (2009) 208-210.

[10] H. Li, X. Pan, M. Qiao, Y. Zhang, T. Wang, and E. Xie. The influence of ambient conditions on properties of MgxZn1-xO films by sputtering. Vacuum, 82 (2008) 459-462.

[11] A. Suryanarayana Reddy, P. Prathap, Y.P.V. Subbaiah, K.T. Ramakrishna Reddy, and J. Yi. Growth and physical behaviour of Zn1-xMgxO films. Thin Solid Films, 516 (2008) 7084-7087.

[12] K. Yoshino, S. Oyama, M. Yoneta, Structural, optical and electrical characterization of undoped ZnMgO film grown by spray pyrolysis method, J. Mat. Sci.: Mat. in Elec. 19 (2008) 203-209.

[13] X. Zhang, X. Min Li, T. L.Chen, J.M. Bian, C. Y. Zhang, Structural and optical properties of Zn1-xMgxO thin films deposited by ultrasonic spray pyrolysis, Thin Solid Films 492 (2005) 248-252.

[14] F. Paraguay D., W. Estrada L., D.R Acosta N., E. Andrade, M. Miki-Yoshida, Growth, structure and optical characterization of high quality ZnO thin films obtained by spray pyrolysis, Thin Solid Films 350 (1999) 192-202.

[15] M. Salou, B. Lescop, S. Rioual, A. Lebon, J. Ben Youssef, B. Rouvellou, Initial oxidation of polycrystalline Permalloy surface, Surf. Sci. 602 (2008) 2901-2906.

[16] T.S. Moss, Semiconductor Opto-electronics, Butterworths, London, 1973.

[17] L.A. Bendersky, I.Takeuchi, K.S. Chang, W. Yang, S. Hullavarad, R.D. Vispute, Microstructural study of epitaxial ZnMgO composition spreads, J. Appl. Phys. 98 (2005) 083526-083532.

[18] Y.F. Lu, H.Q. Ni, Z.H. Mai, Z.M. Ren The effects of thermal annealing on ZnO thin films grown by pulsed laser deposition, J. Appl. Phys. 88 (2000) 498-502.

[19] Y.I. Kim, K. Page, A.M. Limarga, D.R. Clarke, R. Seshadri, Evolution of local structures in polycrystalline Zn1-xMgxO (0=x=0.15) studied by Raman spectroscopy and synchrotron x-ray pair-distribution-function analysis, Phys. Rev. B 76 (2007) 115204-115214.

[20] I.V. Maznichenko, A. Ernst, M. Bouhassoune, J. Henk, M. Däne, M. Lueders, P. Bruno, W. Hergert, I. Mertig, Z. Szotek, Structural phase transitions and fundamental band gaps of MgxZn1- xO alloys from first principles, Phys. Rev. B 80 (2009) 144101-144112.

[21] A. L. Almeida, J. B. L. Martins, and C.A. Taft, J. Chem. Phys. 109 (1998) 3671-3686.

[22] S.E. Ahn, H.J. Ji, K. Kim, G.T. Kim, C.H Bae, S.M. Park, Y.K. Kim, J.S. Ha, Origin of the slow photoresponse in an individual sol-gel synthesized ZnO nanowire, Appl. Phys. Lett. 90 (2007) 153106-153109.

[23] L. Straka, Y. Yagodzinskyy, H. Kawakami, J. Romu, R. Ilola, H. Hänninen, Open-circuit potential as an indicator of damage of atomic layer deposited TiO2 on AISI 304 stainless steel, Thin Solid Films 517 (2008) 641-647.

[24] N.C. Hosking, M.A. Ström, P.H. Shipway, C.D. Rudd, Corrosion resistance of zinc–magnesium coated steel, Corr. Sci. 49 (2007) 3669-3695.

[25] P. Volovitch, C. Allely, K. Ogle, Understanding corrosion via corrosion product characterization: I. Case study of the role of Mg alloying in Zn–Mg coating on steel, Corr. Sci. 51 (2009) 1251-1262.

Figures

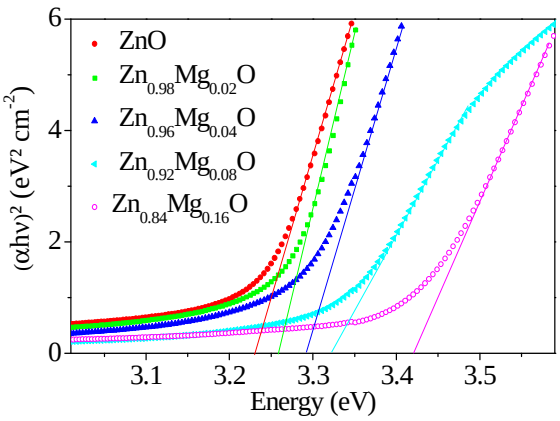

Fig. 1. $\alpha h\nu^2$ versus $h\nu$, optical band gap evolution with Mg doping for $Zn_{(1-x)}Mg_{(x)}O$ (x = 0, 0.02, 0.04, 0.08 and 0.16).

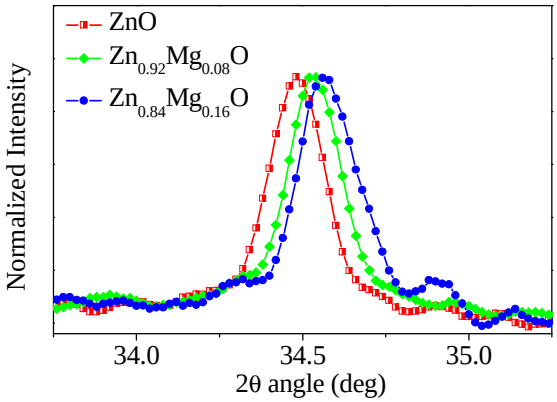

Fig. 2. XRD patterns of ZnO and $Zn_{(1-x)}Mg_{(x)}O$ (002) main peak with Mg doping for x = 0, 0.08 and 0.16.

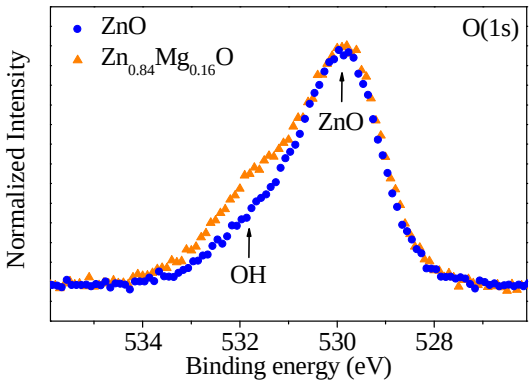

Fig. 3. O(1s) XPS spectra of ZnO and $Zn_{0.84}Mg_{0.16}O$.

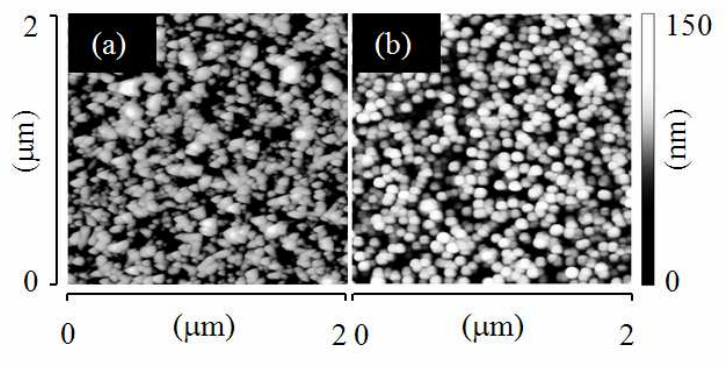

Fig. 4. AFM pictures of ZnO (a) and $Zn_{0.84}Mg_{0.16}O$ (b).

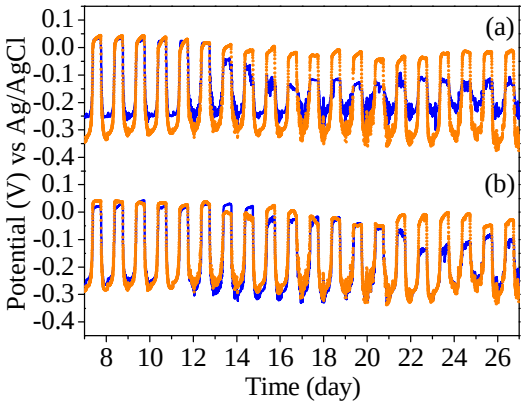

Fig. 5. Open circuit potential of ZnO (full line) and $Zn_{0.84}Mg_{0.16}O$ (dot line) under daylight illumination in borax buffer solution (pH 8.4). (a) daylight exposure (b) 5 days in the dark before exposure to daylight.

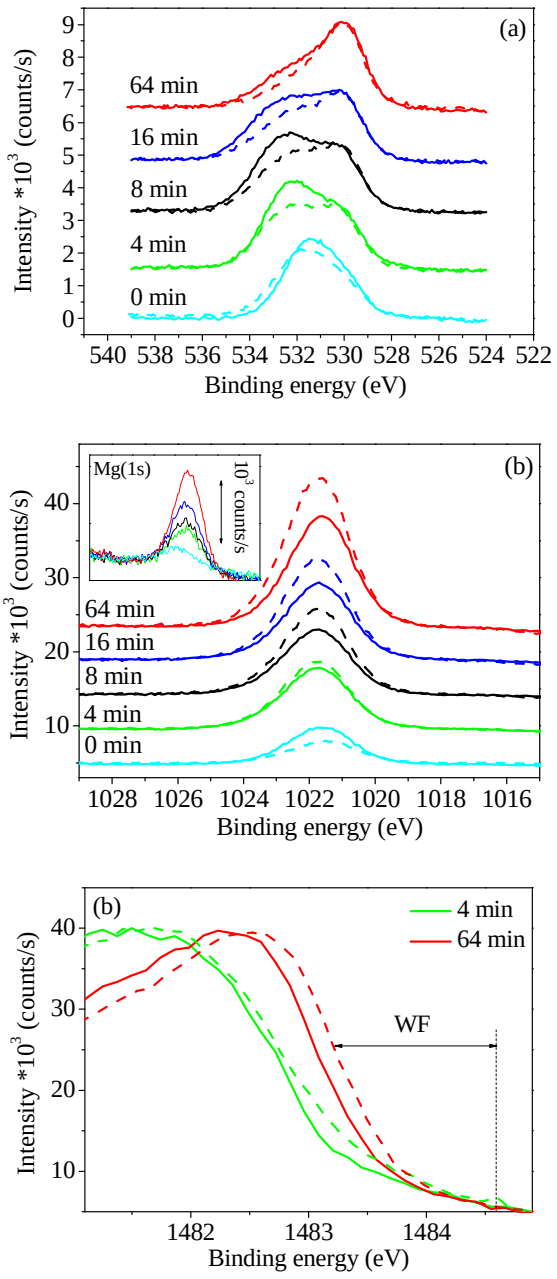

Fig. 6. (a) O(1s) and (b) Zn(2p) XPS spectra of ZnO (dashed line) and $Zn_{0.84}Mg_{0.16}O$ (full line) after exposure to daylight illumination in borax buffer solution (pH 8.4), the inset of (b)

represents the Mg(1s) spectra; (c) secondary electrons spectra measurements of ZnO (dashed line) and ZnMgO (full line).